Journal of Analytical Atomic Spectrometry

Estimating the grade of Mg corrosion using Laser-Induced Breakdown Spectroscopy

Journal:	*Journal of Analytical Atomic Spectrometry*
Manuscript ID:	JA-ART-07-2015-000257.R1
Article Type:	Paper
Date Submitted by the Author:	23-Jul-2015

Complete List of Authors:	Pořízka, Pavel; Central European Institute of Technology Brno University of Technology (CEITEC BUT), Ročňáková, Ivana; Central European Institute of Technology Brno University of Technology (CEITEC BUT), Klus, Jakub; Central European Institute of Technology Brno University of Technology (CEITEC BUT), Prochazka, David; Central European Institute of Technology Brno University of Technology (CEITEC BUT), Sládková, Lucia; Central European Institute of Technology Brno University of Technology (CEITEC BUT), Šperka, Petr; Faculty of Mechanical Engineering Brno University of Technology, Spotz, Zdeněk; Central European Institute of Technology Brno University of Technology (CEITEC BUT), Čelko, Ladislav; Central European Institute of Technology Brno University of Technology (CEITEC BUT), Novotný, Karel; Central European Institute of Technology Brno University of Technology (CEITEC BUT), Kaiser, Jozef; Central European Institute of Technology Brno University of Technology (CEITEC BUT),

SCHOLARONE™
Manuscripts

Journal of Analytical Atomic Spectrometry

ARTICLE

Estimating the grade of Mg corrosion using Laser-Induced Breakdown Spectroscopy

Received 00th January 20xx,
Accepted 00th January 20xx

DOI: 10.1039/x0xx00000x

www.rsc.org/

P. Pořízka[a,†], I. Ročňáková[a], J. Klus[a], D. Prochazka[a], L. Sládková[a], P. Šperka[b], Z. Spotz[a], L. Čelko[a], K. Novotný[a,c], J. Kaiser[a,b]

We present a report on the potential use of Laser-Induced Breakdown Spectroscopy (LIBS) technique for direct investigation of Mg corrosion and related optimization of table-top LIBS system. Moreover, the preliminary study to prove the capability of LIBS technique for the estimation of corrosion grade is given. In order to simulate the real corrosive environment, Mg samples were prepared in the constant climate chamber. We show that the corrosive layer on the sample surface significantly affects properties of laser-matter interaction, *i.e.* among other parameters causes the matrix effect. Consequently, the properties and persistence of laser-induced plasmas (LIPs) and their composition, generated on such degraded surfaces, essentially differ. Collected radiation of LIP is then analysed and ratios of ionic to atomic Mg spectral lines are correlated with the grade of magnesium corrosion, *i.e.* content of $Mg(OH)_2$ on the sample surface. The content of $Mg(OH)_2$ is also correlated with plasma temperature as well as with the electron number density of LIP. Additionally, X-ray diffraction (XRD) analysis and optical profilometry were utilized to obtain more comprehensive information about the degradation grade of high purity Mg samples.

Introduction

Magnesium and magnesium alloys are promising materials in the automotive and aerospace industry due to their low density and high strength-to-weight ratio [1]. Mg density is 1.74 $g.cm^{-3}$, only 2/3 that of aluminium and 1/4 that of iron. Furthermore, it has also many advantageous properties such as excellent machinability, good electromagnetic shielding characteristics, recyclability and biocompatibility, *etc.* Therefore, magnesium and its alloys have the potential to replace steel and aluminium in many applications. The main disadvantage of Mg alloys, their poor corrosion resistance, was found useful in certain biomedical applications, for instance in orthopaedics for bone scaffolding [2], where the scaffold is composed of Mg alloy and naturally decays away with simultaneous growth of the bone. Magnesium is extremely sensitive to impurity elements such as Fe, Ni, Cu and Co in terms of the corrosion performance. Magnesium based metals are generally known to get corroded in an aqueous environment via an electrochemical reaction, which produces magnesium hydroxide and hydrogen gas.

In case of Mg corrosion in NaCl solution, it is well known that singly ionized Cl easily induces pitting corrosions [3]. When the chloride concentration in the corrosive environment rises above 30 mmol/L, magnesium hydroxide is formed and reacts with magnesium to form highly soluble magnesium chloride and thus the degradation rate is increased. The corrosion of magnesium is mainly localized, leading to the formation of cracks and pits.

Corrosion behaviour is usually monitored by the sample weight loss (after removal of corrosion products), measurement of pH and X-Ray diffraction (XRD). Corrosion behaviour could be also characterized by hydrogen evolution and electrochemical measurements (electrochemical polarization curves, electrochemical impedance spectroscopy). Sample surface morphology can be studied by optical microscope and scanning electron microscope (SEM) and its composition by SEM energy dispersive X-ray analysis (EDX) [4 - 7].

Materials exposed to aggressive environment undergo certain changes in their composition, leadind to degradation of their mechanical properties (endurance, flexibility, *etc.*). Such degradation processes in metals, for instance corrosion, of metals are well understood and described [8, 9]. Moreover, in certain applications it is advantageous to control the material quality remotely. Thus, measurement of materials in difficult-to-reach places is an insuperable task for many conventional methods.

Laser-Induced Breakdown Spectroscopy (LIBS) is able to yield its position among other spectroscopic techniques for its capability of real-time corrosion grade estimation in different materials. In general, LIBS [10, 11] is a technique based on

[a] CEITEC BUT, Central European Institute of Technology, Brno University of Technology, Technická 3058/10, 61600 Brno, Czech Republic.
[b] Faculty of Mechanical Engineering, Brno University of Technology, Technická 2896/2, 61669 Brno, Czech Republic.
[c] CEITEC MU, Central European Institute of Technology, Masaryk University, Kamenice 753/5, 65200 Brno, Czech Republic
† Corresponding author, pavel.porizka@ceitec.vutbr.cz
See DOI: 10.1039/x0xx00000x

This journal is © The Royal Society of Chemistry 20xx

Please do not adjust margins

atomic emission spectroscopy (AES) with advantages such as cost-effective analysis, robust instrumentation, and even *in-situ* and stand-off sensing. LIBS has already been used in vast variety of applications, *e.g.* in industry [12], geology [13], cultural heritage [14], biomedical [15] and biological applications [16 - 18], and also for *in-situ* analysis [19] [20]. The comprehensive review on LIBS applications was brought by Hahn and Omenetto [21]. Briefly, a short high energy laser pulse is focused into a tight spot on the sample surface to be analysed. Then, a small amount of the sample is melted, evaporated, atomized and ionized; *i.e.* the laser-induced plasma (LIP) is generated. LIBS technique is based on the analysis of spectral features of detected atomic and ionic radiation of luminous LIP. A typical LIP spectrum is composed of characteristic radiation of ablated species, the so-called chemical fingerprint. Therefore, detected LIP spectra may then be utilized for qualitative, quantitative analysis and classification [10]. Despite its advantages, LIBS gets significantly affected by the matrix effect as well as other analytical techniques based on laser ablation process [10, 21]. This means that the generated LIP is influenced by variances in the target physical properties and its elemental composition. For that reason the quantitative analysis employing LIBS technique is challenging and standardized series of matrix matched samples are needed in order to calibrate the system for the selected application.

It was shown that surface composition of archaeological findings affects analytical results [22]. The analysis of ancient metallic objects, pottery, *etc.* has to be done with care to avoid corrosion products. Consecutive laser pulses may be used to clean the surface. The presence of corrosion on those surfaces is of a great importance. As the results may not be representing the bulk of the target. Depth profiling analysis is useful in the study of composition and content of corrosion products on the sample surface.

Elhassan and Harith [23] brought a brief review on LIBS for corrosion diagnostics with the emphasis on archaeological findings and art objects as well as steel parts employed in harsh industrial environments. Moreover, it is beneficial to use more techniques in tandem in order to obtain comprehensive information about the investigated samples. Pérez-Serradilla *et al.* [24] tested the complementarity of LIBS and X-ray fluorescence (XRF) techniques on the set of 18^{th} century ancient coins. XRF was applied prior to the LIBS analysis, when the main emphasis of the experimental work was put on LIBS optimization and detection. The authors suggested that the increase in corrosion products on the sample surface decreases the intensity of atomic lines. Consequently, the intensity of an atomic line increases with the increase of laser pulses on the same spot in a depth profiling experiment. Alberghina *et al.* [25] employed LIBS with SEM to improve the understanding of corrosion processes of archaeological samples. Furthermore, the provenance of various bronze samples was estimated based on their LIP spectral information.

Schlegel *et al.* [26] utilized several microscopic and spectroscopic techniques (such as SEM-EDX, Raman spectroscopy, XRF and LIBS) on a micro-scale to study temporal phase changes in iron-clay interface. Maps of elemental distribution delivered from LIBS and SEM-EDX data were comparable, with the emphasis on Na, Mg, Al, Si, Ca, and Fe. Moreover, the performance of LIBS in the detection of Na was significantly better with respect to XRF analysis.

Another application of LIBS for direct *in-situ* analysis is the monitoring of metallic corrosion in industrial processes. Kim *et al.* [27] analysed Ni-based superalloys for very high temperature reactors by LIBS, SEM-EDX, XRD and secondary ion mass spectrometry (SIMS). Selected techniques were utilized together in order to compare their analytical performance. LIBS was performed to check the depth-profile of Ni, Cr, Mn, and Al in samples with different grades of corrosion. The surface morphologies of samples analysed by SEM-EDX were in good agreement with depth-profiling measurements provided by LIBS.

Bulajic *et al.* [28] carried out space-resolved elemental analysis of high-temperature steel pipes using LIBS directly in industrial environments. The authors proposed the design of a laser head specifically for harsh environments. However its applicability was tested only in laboratory conditions. On the other hand, the challenges arising with the positioning of a robust laser head may be avoided by using a stand-off LIBS system. García *et al.* [29] measured the high-temperature corrosion of stainless steel with open-path LIBS device at a distance of 10 m. The steel samples were exposed to various temperatures and then the changes in their surface composition were investigated. Simultaneously, the system was utilized in the depth-profiling mode to check the deepening of corrosion products. This feasibility study proved the capability of the stand-off LIBS technique to analyse the depth profile of corrosive layers.

We have already studied and proposed an experimental algorithm allowing the matrix effect correlation (*i.e.* varying hardness of bricks) with selected spectral features in our previous paper [30]. Several bricks samples were analysed using table-top and stand-off LIBS systems. The firing temperature of selected samples was successfully correlated with the intensity ratio of Mg ionic to atomic lines. Hence, the systematic changes in intensities of Mg lines were affected by the matrix effect. The higher the firing temperature, the higher the intensity ratio of Mg II to Mg I lines. Consequently, the firing temperature may be estimated from the Mg II to Mg I lines ratio. Furthermore, the provenance study of brick samples was provided based on the differences in LIP spectral features utilizing the principal component analysis and linear discriminant analysis.

In this article, we proved the possibility to estimate Mg corrosion grade from the changes in spectral features of LIBS measurements. The amount of $Mg(OH)_2$ was successfully correlated with the detected LIP spectra. The matrix effect was adapted in respect to ionic to atomic spectral lines ratio. Plasma temperature and electron number density were estimated and successfully correlated with the amount of $Mg(OH)_2$ products. At the same time, the analytical

This journal is © The Royal Society of Chemistry 20xx

information from XRD was obtained to check the competitiveness of LIBS analysis.

Experimental

Samples

High purity magnesium (HP-Mg, 99.9%, Goodfellow) discs (12.7 mm in diameter x 5 mm in height) used in this study were cut from an extruded rod. While the surfaces perpendicular to the disc axes were mechanically polished using SiC papers ranging from 320 to 1000 grits, the disc edges were not pre-treated in any way. Afterwards, the HP-Mg discs were aged under controlled conditions. HP-Mg was corroded by immersion in 0.9 wt.% NaCl solution of analytical grade chemical (G.R. grade purity; Lach-Ner, Czech Republic) and distilled water. During the experiments, the temperature of the test solution was controlled in the constant climate chamber KMF 115 (Binder, Germany) at 30±1°C during 1 to 4 weeks.

LIBS

HP-Mg and corroded Mg samples were analysed using table-top LIBS, described also in ref. [18]. High energy Nd:YAG laser LQ 529A (Solar LS, Belarus) operated at its second harmonic wavelength (532 nm, 30 mJ, 10 Hz, 10 ns) was utilized. Laser pulse was introduced into the LIBS interaction chamber (AtomTrace, Czech Republic), described in detail in [31], by a series of mirrors (ThorLabs, USA) and then focused onto the sample surface with coated plano-convex lens (50 mm, ThorLabs, USA). The diameter of the resulting laser spot on the HP-Mg surface was 80 µm. Thus, the irradiance of the laser pulse in interaction region was approximately 60 GW.cm^{-2}. Samples were placed on the precise positioning table within the LIBS interaction chamber. The sample stage was moved before each laser pulse to provide fresh spot for the consecutive LIBS analysis. Radiation of luminous LIP was collected with optimized doublet and via optical fibre (Ø40 µm, Thorlabs, USA) coupled to an echelle spectrometer Mechelle 5000 (Andor, UK; 200 – 975 nm, F/7, 6000 λ/Δλ). Collection optics was positioned under the angle of 66° in respect to ablation laser axis and in the distance of 80 mm from the interaction region. Spectrally resolved radiation was then recorded with ICCD camera iStar 734i (Andor, UK; 1024 x 1024 pixels, effective pixel size 19.5 x 19.5 µm). The 20 µs gate width of the ICCD was set 1.5 µs after firing the laser pulse (gate delay), the optimization process is shown later in the text. In the experiment, thin corroded layers of 5 Mg samples (with the same corrosion grade) were measured. For each sample 10 laser pulses were utilized with no accumulation and a fresh spot was provided for each consecutive laser pulse. Detected LIP spectra during the LIBS measurements were analysed in the commercially available software AtomAnalyzer (AtomTrace, Czech Republic), specifically developed for LIBS applications. Selected characteristic spectral lines of Mg were fitted with Voigt profiles and the areas under the fitted curve with background subtraction were taken as the signal intensity. Intensity of selected analytical line was normalized using LIP emission signal integrated over the whole detected spectrum. Afterwards, all measured spectra of individual samples averaged.

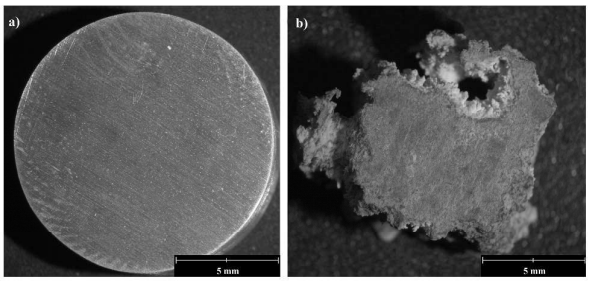

Figure 1: Top-bottom view on a) HP-Mg sample and b) sample with corrosion products after 4 weeks of ageing

Additional methods

The parameters of LIBS craters (their depth and diameter) were estimated using the optical microscope Contour GT-X (Bruker, Germany). X-Ray diffraction based phase analysis was performed from a diffraction pattern measured on the flat surface of prepared samples. XRD was measured at 3 kW diffractometer Smartlab (Rigaku, Japan). The diffractometer equipped with 1D detector Dtex Ultra was set up in the Bragg-Brentano geometry using Cu K-alpha radiation (λ = 1.54 Å). Cu lamp was operated at 30 mA current and 40 kV voltage. The diffracted area on the surface of the specimen was about 1 cm^2, the penetration depth for analysed material and used X-ray source is in the order of tens of micrometers. Phase analysis was performed based on the chemical composition expected from the corrosion process using databases PDF2 and ICSD. Qualitative phase analysis was calculated by the Rietveld refinement from measured powder diffraction data using the external Si standard. Peak profiles were fitted by the pseudo-Voigt function and the background was refined with the polynomial function of 5th order. XRD measurements were performed in order to control the analytical performance of the LIBS systems.

Results

Preliminary analysis

HP-Mg samples degraded in the constant climate chamber were significantly affected by corrosion. As it is depicted in the Figure 1, the corrosion has distinctly different effect on the circumference and the top surfaces. This phenomenon is a result of fabrication of HP-Mg rod, which the experimental samples were cut from. LIBS and XRD measurements were realized on the top and bottom surfaces of degraded Mg samples where the corrosion layer is more uniform. Therefore, it was supposed that the shot-to-shot LIBS measurements will be reproducible and intra- and inter-comparable.

The phase compositions and phase structures of HP-Mg were determined using XRD analysis. The structural changes of HP-

This journal is © The Royal Society of Chemistry 20xx

Please do not adjust margins

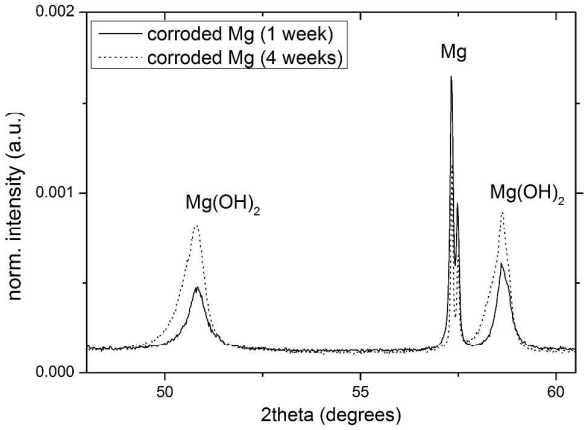

Figure 2: Section of typical XRD spectra used in analysis

Mg using the XRD analysis are represented by the differences in Mg and $Mg(OH)_2$ peak intensities, shown in Figure 2. The XRD results indicate that the surface layer of corrosion products consists mainly of $Mg(OH)_2$. After 1 week, a porous deposit layer was formed at some regions on the surface of the sample. This deposit increased with immersion time and it covered the entire sample surface in 4 weeks. The intensity of $Mg(OH)_2$ peaks increases with increasing time of immersion in aggressive environment; that corresponds to increasing amount of $Mg(OH)_2$ on the surface of the specimen. Therefore, the content of $Mg(OH)_2$ was assigned to the grade of Mg corrosion.

Based on the assumption that changes in the surface composition affect its mechanical properties, we attempted to measure micro- and nanohardness of the corrosive products. Nevertheless, the attempts to estimate the nanohardness were not successful. The microhardness measurements of corroded layer resulted in the same value of microhardness as measured on HP-Mg sample. Those unsuccessful attempts were probably caused by the softness and thinness of corroded layers. Therefore, the analytical results obtained using LIBS and XRD could not be correlated with the mechanical properties of degraded layers formed on the surfaces of Mg samples. It was not possible to check the consistency of the results with the experimental work of Labutin *et al.* [32], where microhardness of aluminium alloys was correlated with temperature of LIP estimated using Li emission lines.

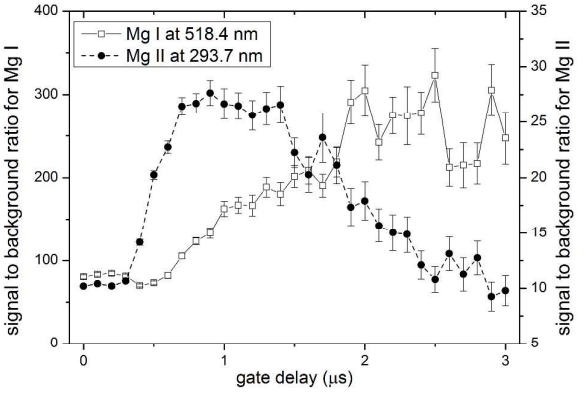

Figure 3: Dependence of atomic and ionic Mg emission line intensities on gate delay

LIBS analysis

As mentioned above, LIP evolves rapidly spatially and temporally during its short persistence (usually units to tens of μs). However, the analytically valuable detected radiation is, in the beginning of LIP, a temporal evolution degraded by the inverse Bremsstrahlung and the continuum radiation. This disruptive radiation vanishes after several hundreds of nanoseconds. Therefore, it is necessary to optimize the LIBS system prior to the analysis to obtain the best possible performance of the system. In other words, the detection window of the ICCD has to be delayed with respect to the beginning of LIP formation. In practice, the LIBS system is step-wise optimized for the best signal to background ratio (SBR). Intensity of the selected analytical line was considered as the signal and close proximity of this line was assumed as the background, as explained thoroughly elsewhere [33]. The optimization process was executed on HP-Mg sample. In Figure 3 the gate delay was varied in steps of 100 ns in the span of 3 μs and the signals of Mg I line (518.4 nm) and Mg II line (293.7 nm) are divided by the background intensity in their close proximity. In the beginning, LIP is strongly ionized, which is reflected in Figure 5 by a more intense ionic line which vanishes after 2.5 μs. Afterwards, the radiation of atomic line is increased as the ions recombine with electrons and the composition of LIP gets atomized. The SBR for atomic line reaches its maximum at 2 μs and then levels off. Therefore, the optimum conditions for the table-top LIBS experiment were set to 1.5 μs, where the slopes of SBRs for atomic and ionic line are high and thus sensitive to fluctuations. The width of detection window, *i.e.* gate width, was set to 20 μs throughout the LIBS analysis to detect complete radiation of LIP.

It is known that techniques based on laser-ablation are significantly affected by the so-called matrix effect [10, 11]. Therefore, various conditions of laser-matter interaction will

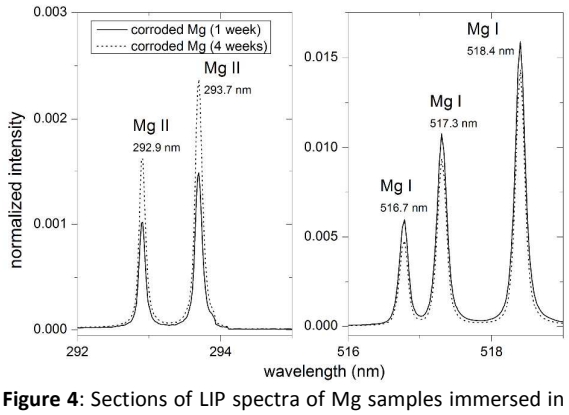

Figure 4: Sections of LIP spectra of Mg samples immersed in corrosive environment for 1 and 4 weeks respectively

This journal is © The Royal Society of Chemistry 20xx

Please do not adjust margins

vastly influence the material ablation process, dynamics of LIP spatial and temporal evolution and the intensity of atomic and ionic lines radiation respectively. In our experiment, samples with various corrosion grades (*i.e.* various contents of matrix components in Mg and $Mg(OH)_2$) were selected and analysed under the same experimental LIBS conditions. Consequently, the properties of generated LIPs on particular samples differ due to the influence of matrix effect. Therefore, the system was optimized using HP-Mg sample and subsequently the corroded samples were analysed. It is important to keep the experimental conditions stable and vary only the matrices of samples, *i.e.* corrosion grades. Thus, it is possible to estimate the material degradation grade from the differences in atomic to ionic lines ratios in corresponding LIPs spectra.

The experimental conditions were maintained constant during the analysis of corroded Mg samples. The influence of laser energy fluctuations on the laser-matter interaction was neglected because the stability of Mg lines signals in the pulse-to-pulse analysis of homogeneous HP-Mg sample was well below 1%. Therefore, surface composition inhomogeneity, hence possible variations in surface roughness and hardness, were identified as the main sources of signal fluctuations in Mg corrosion measurements. Based on relative standard deviations of analytical lines it is reasonable to conclude that the main source of variation in the laser-matter interaction is the amount of corrosion products ($Mg(OH)_2$ content) formed on the samples surfaces.

Despite the fact that microhardness and nanohardness measurements were not successful, it is reasonable to expect that physical properties (sample matrix: hardness, roughness, reflectivity, *etc.*) of the sample surface will change with the content of $Mg(OH)_2$. This significantly impacts the ablation process. Concerning the ablation process, a significantly higher amount of energy is necessary to melt and vaporize the sample than to heat up and ionize the vapour [11]. The melting point of $Mg(OH)_2$ is at 623 K while the melting point of Mg is at 923 K. On the other hand, the heat capacity of $Mg(OH)_2$ and Mg is approximately at 77 J/mol.K and 25 J/mol.K respectively. Based on the above-mentioned physical properties of both materials, it is expectable that more energy would be used for ionization of $Mg(OH)_2$ sample. That is in contradiction with presented results. This may in turn correspond to the lower ablation threshold of $Mg(OH)_2$ in respect to the one of HP-Mg.

Table 1: List of Mg lines utilized for estimation of LIP parameters

line	λ_{ref} [nm]	g_kA_{ki} [$.10^8$ s^{-1}]	E_k [eV]
Mg I	309.30	1.87	6.72
Mg I	309.69	3.47	6.72
Mg I	382.94	2.7	5.95
Mg I	383.23	6.05	5.95
Mg I	516.73	0.34	5.11
Mg I	517.27	1.01	5.11
Mg I	518.36	1.68	5.11
Mg I	571.11	0.039	6.52
Mg II	292.86	2.3	8.65
Mg II *	293.65	4.6	8.65
Mg II	448.13	18.6	11.63

*line was utilized for the computation of electron number density

With regards to the theory, measurement of HP-Mg was omitted from this manuscript. It has significantly different sample matrix giving high intensity ratio of Mg II to Mg I. On the contrary, sample matrix consisting of HP-Mg and $Mg(OH)_2$ mixture is affected also by variations in physical properties.

Additionally, the intensities of atomic and ionic lines strongly differ within the observed spectra of various grades of Mg corrosion. As it may be seen in Figure 4, there is a significant difference in LIP spectra for neutral and singly ionized Mg lines detected in LIPs of corroded targets. This is a consequence of LIP persistence and its properties influenced by a different laser-matter interaction. Therefore, the ratio of ionic to atomic Mg lines was utilized for estimation of Mg corrosion. The emission intensity of ionic Mg II line at 293.7 nm is divided by the intensity of atomic Mg I line at 518.4 nm, not shown. The observed trend suggests that it is possible to calibrate a table-top LIBS system for this kind of analysis. In other words, it is possible to relate the LIP spectral features with material degradation and hence the immersion time in a corrosive environment. Moreover, from Figure 5 it is obvious that the longer the immersion time, i.e. the bigger the amount of

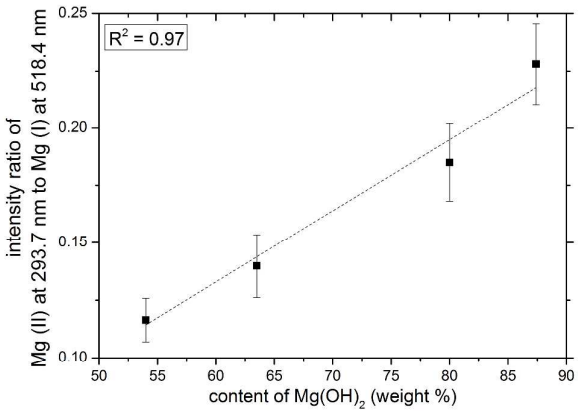

Figure 5: Calibration of LIBS system for the analysis of Mg corrosion grades based on the content of $Mg(OH)_2$

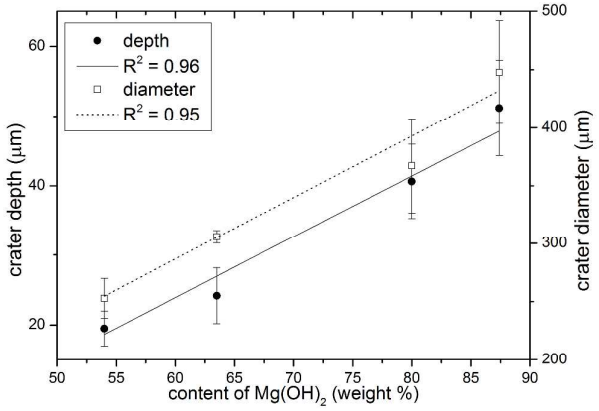

Figure 6: Crater parameters in LIBS experiment as a function of $Mg(OH)_2$ content

Please do not adjust margins

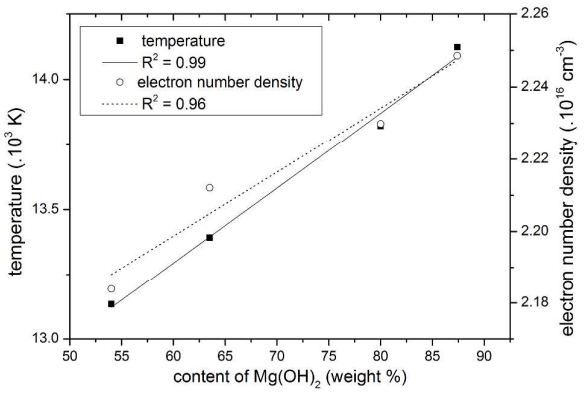

Figure 7: Temperature and electron number density

corrosion products, the higher the intensity of ionic Mg II line at 293.7 nm and ionic Mg lines in general. Therefore, it is reasonable to expect that the temperature of LIP gets higher with the amount of corrosion. As stated above, the melting point of $Mg(OH)_2$ is lower than that of Mg. In other words, the conditions for laser-matter interaction are more favourable for generation of LIP on the sample with a longer immersion time.

During the optimization process, the diameter of the ablated crater was 80 µm. However, the diameters of ablated craters on corroded samples were significantly wider, as can be seen in Figure 6. This may be explained by the change in the amount of corrosion products, *i.e.* the $Mg(OH)_2$ content, and consequently the properties of surfaces of investigated samples. The possible explanation is thickness and poor consistency (hardness) of the corroded layer; was easily removed manually. Nevertheless, the trend observed in this figure represents deepening and widening of the ablated crater with an increasing content of corrosion products. Naturally, a lower melting point of $Mg(OH)_2$ may result in a higher ablated volume.

As it was mentioned in the introduction, LIBS technique offers a pulse-to-pulse analysis with a depth resolution, *i.e.* depth profiling. Therefore, it is possible to obtain information about the elemental composition under the sample surface utilizing consecutive laser pulses into the same spot, *i.e.* interaction region. Consequently, it is possible to monitor deepening of the material corrosion. Regarding mechanical properties of the corrosion products, our attempts to run any depth profiling analysis of corroded surfaces using LIBS failed. After the first laser pulse, only the base matrix was present in the interaction region.

The matrix effect significantly affects the LIP properties (such as temperature and electron number density) [10, 11]. Determination of those parameters is well described in literature [34 - 36] and their estimation is not to be explained here thoroughly. Firstly, the electron number density was calculated from broadening of Mg II line at 293.7 nm. The spectral line broadening is caused only by the Stark broadening effect (causing the Lorentzian line profile) and contributions from Doppler and instrumental broadenings (causing Gaussian line profile) [11]. As may be found in literature [36], the Stark effect is considered to be the main factor of line broadening. However for further computation of electron number density, the spectral line was fitted with the Voigt profile to reflect the contributions from both, Gaussian and Lorentzian, broadenings. The electron impact value ω for Mg II line at 293.7 nm is 0.0134, as taken from [37]. Then, the spectral width of the selected spectral line, obtained from the Voigt fit, in samples with various Mg corrosion grades may be directly utilized for estimation of the electron number density. Additionally, plasma temperature was calculated using the Saha-Boltzmann plot from intensities of neutral and singly ionized Mg spectral lines, obtained from [38] and listed in Table 1, where λ_{ref} is NIST reference wavelength (nm), g_k is the degeneracy of the upper level, A_{ki} is the transition probability (s^{-1}) and E_k is the energy of the upper level (eV). In the computation, the upper level energy of singly ionized Mg species is corrected by the ionization energy, 7.64 eV for Mg. In the Saha-Boltzmann method, the electron number density is obtained from the spectral line broadening and introduced into the equation. Hence, the plasma temperature is iterated using the procedure based on the ion correction form, as explained elsewhere [34].

Obtained values of plasma temperature and electron number density are plotted in Figure 7 as a function of $Mg(OH)_2$ content. It is visible that the plasma temperature and electron number density are correlated with the increasing content of $Mg(OH)_2$ products on degraded sample surfaces. Both dependencies suggest an influence of the amount of corrosion products on the dynamics of ablation processes and hence on the LIP formation. Therefore, it is reasonable to expect that such changes in the matrix composition soften the sample surface and consequently enable easier formation of LIPs. It should be however noted that these results have to be accepted carefully, while the computation is significantly affected by error. The standard deviation which is observed in such computations may reach up to 50% [10]. Concerning the relative standard deviation of temperature and electro number density values in the range from 10 to 15%, they are a consequence of high relative deviations of tabulated values, as stated by Aguilera and Aragón [34].

Conclusions

In this feasibility study we have proven the capability of a table-top LIBS system to perform direct estimation of Mg corrosion grade. Moreover, performance of the utilized LIBS system was obtained with the coefficient of determination above 97%. In the first instances, it is necessary to control the performance of LIBS using other well-established analytical methods, such as XRD in the case of presented work. However, having matrix matched standards and calibrating the LIBS system for a certain task it would be possible to run the LIBS analysis *in-situ* and even in a stand-off mode with no need for other supporting analytical methods. This will lead to acceleration and effectivity in the direct analysis of corrosion products.

The results of the LIBS analysis were in a good conformity with XRD measurements, where the content of $Mg(OH)_2$ was rising

 This journal is © The Royal Society of Chemistry 20xx

Please do not adjust margins

with the interval of immersion and the value of Mg II to Mg I intensity ratio respectively. The LIP temperature and electron number density as well as the LIBS crater sizes are increasing with the Mg corrosion grade, *i.e.* content of $Mg(OH)_2$. The presented results and literature research suggest that with increasing $Mg(OH)_2$ content the surface hardness is decreasing. To reach a conclusion based on this feasibility study, it is possible to obtain reliable results, *i.e.* estimate the corrosion grade of metals, by the means of LIBS sensing.

Acknowledgements

We acknowledge the support from the project "CEITEC – Central European Institute of Technology" (CZ.1.05/1.1.00/02.0068) from the European Regional Development Fund. L.S. would like to acknowledge the support by the project "CEITEC — Central European Institute of Technology" within the framework of the grant STI-S-14-2523 (Advanced Nanotechnologies and Materials). P.Š. and J. Ka. acknowledge the projects FSI-S-14-2336 and FSI-S-14-2494, respectively from the Ministry of Education, Youth and Sports.

References

[1] E. Czerwinski, Magnesium alloys: corrosion and surface treatments. Rijeka: InTech, 2011.

[2] M. Staiger, A. Pietak, J. Huadmai and G. Dias, "Magnesium and its alloys as orthopedic biomaterials: A review", Biomaterials, vol. 27, no. 9, pp. 1728-1734, 2006.

[3] L. Tan, X. Yu, P. Wan and K. Yang, "Biodegradable Materials for Bone Repairs: A Review", Journal of Materials Science, vol. 29, no. 6, pp. 503-513, 2013.

[4] G. Song, "Control of biodegradation of biocompatable magnesium alloys", Corrosion Science, vol. 49, no. 4, pp. 1696-1701, 2007.

[5] G. Song, A. Atrens, X. Wu and B. Zhang, "Corrosion behaviour of AZ21, AZ501 and AZ91 in sodium chloride", Corrosion Science, vol. 40, no. 10, pp. 1769-1791, 1998.

[6] Y. Xin, C. Liu, X. Zhang, G. Tang, X. Tian and P. Chu, "Corrosion behavior of biomedical AZ91 magnesium alloy in simulated body fluids", Journal of Materials Research, vol. 22, no. 07, pp. 2004-2011, 2007.

[7] E. Zhang, L. Yang, J. Xu and H. Chen, "Microstructure, mechanical properties and bio-corrosion properties of Mg–Si(–Ca, Zn) alloy for biomedical application☆", Acta Biomaterialia, vol. 6, no. 5, pp. 1756-1762, 2010.

[8] G. Song, ed., Corrosion of magnesium alloys, 1st ed. Cambridge: Woodhead, 2011, p. xxiii, 640 s.

[9] G. Song, Corrosion prevention of magnesium alloys. Philadelphia: Woodhead Publishing, 2013, p. xix, 562 p.

[10] A. Miziolek, V. Palleschi and I. Schechter, Laser Induced Breakdown Spectroscopy. Cambridge: Cambridge University Press, 2006.

[11] R. Noll, Laser-induced breakdown spectroscopy fundamentals and applications, 2012. Heidelberg: Springer-Verlag Berlin Heidelberg, 2012.

[12] R. Noll, C. Fricke-Begemann, M. Brunk, S. Connemann, C. Meinhardt, M. Scharun, V. Sturm, J. Makowe and C. Gehlen, "Laser-induced breakdown spectroscopy expands into industrial applications", Spectrochimica Acta Part B: Atomic Spectroscopy, vol. 93, pp. 41-51, 2014.

[13] R. Harmon, R. Russo and R. Hark, "Applications of laser-induced breakdown spectroscopy for geochemical and environmental analysis: A comprehensive review", Spectrochimica Acta Part B: Atomic Spectroscopy, vol. 87, pp. 11-26, 2013.

[14] R. Gaudiuso, M. Dell'Aglio, O. Pascale, G. Senesi and A. De Giacomo, "Laser Induced Breakdown Spectroscopy for Elemental Analysis in Environmental, Cultural Heritage and Space Applications: A Review of Methods and Results", Sensors, vol. 10, no. 8, pp. 7434-7468, 2010.

[15] S. Rehse, H. Salimnia and A. Miziolek, "Laser-induced breakdown spectroscopy (LIBS): an overview of recent progress and future potential for biomedical applications", Journal of Medical Engineering, vol. 36, no. 2, pp. 77-89, 2012.

[16] D. Santos, L. Nunes, G. de Carvalho, M. Gomes, P. de Souza, F. Leme, L. dos Santos and F. Krug, "Laser-induced breakdown spectroscopy for analysis of plant materials: A review", Spectrochimica Acta Part B: Atomic Spectroscopy, vol. 71-72, pp. 3-13, 2012.

[17] J. Kaiser, K. Novotný, M. Martin, A. Hrdlička, R. Malina, M. Hartl, V. Adam and R. Kizek, "Trace elemental analysis by laser-induced breakdown spectroscopy—Biological applications", Surface Science Reports, vol. 67, no. 11-12, pp. 233-243, 2012.

[18] P. Pořízka, P. Prochazková, D. Prochazka, L. Sládková, J. Novotný, M. Petrilak, M. Brada, O. Samek, Z. Pilát, P. Zemánek, V. Adam, R. Kizek, K. Novotný and J. Kaiser, "Algal Biomass Analysis by Laser-Based Analytical Techniques—A Review", Sensors, vol. 14, no. 9, pp. 17725-17752, 2014.

[19] F. Fortes, J. Moros, P. Lucena, L. Cabalín and J. Laserna, "Laser-Induced Breakdown Spectroscopy", Analytical Chemistry, vol. 85, no. 2, pp. 640-669, 01 2013.

[20] J. Rakovský, P. Čermák, O. Musset and P. Veis, "A review of the development of portable laser induced breakdown spectroscopy and its applications", Spectrochimica Acta Part B: Atomic Spectroscopy, vol. 101, pp. 269-287, 2014.

[21] D. Hahn and N. Omenetto, "Laser-Induced Breakdown Spectroscopy (LIBS), Part II: Review of Instrumental and Methodological Approaches to Material Analysis and Applications to Different Fields", Applied Spectroscopy, vol. 66, no. 4, pp. 347-419, 04 2012.

[22] C. Fotakis, D. Anglos, V. Zafiropulos, S. Georgiou and V. Tornari, Lasers in the preservation of cultural heritage: principles and applications. New York: Taylor, c2007, p. 336 p.

[23] A. Elhassan, "Short Review Of Laser-Induced Breakdown

This journal is © The Royal Society of Chemistry 20xx

Please do not adjust margins

Spectroscopy For Corrosion Diagnostic", AIP Conference Proceedings, vol. 1380, pp. 65-69, 2011.

[24] J. Pérez-Serradilla, A. Jurado-López and M. Luque de Castro, "Complementarity of XRFS and LIBS for corrosion studies", Talanta, vol. 71, no. 1, pp. 97-102, 01 2007.

[25] M. Alberghina, R. Barraco, M. Brai, L. Pellegrino, F. Prestileo, S. Schiavone and L. Tranchina, "Gilding and pigments of Renaissance marble of Abatellis Palace: non-invasive investigation by XRF spectrometry", X-Ray Spectrometry, vol. 42, no. 2, pp. 68-78, 2013.

[26] M. Schlegel, C. Bataillon, K. Benhamida, C. Blanc, D. Menut and J. Lacour, "Metal corrosion and argillite transformation at the water-saturated, high-temperature iron–clay interface: A microscopic-scale study", Applied Geochemistry, vol. 23, no. 9, pp. 2619-2633, 2008.

[27] T. Kim, D. Lee, D. Kim, C. Jang and J. Yun, "Analysis of oxidation behavior of Ni-base superalloys by laser-induced breakdown spectroscopy", Journal of Analytical Atomic Spectrometry, vol. 27, no. 9, pp. 1525-, 2012.

[28] D. Bulajic, G. Cristoforetti, M. Corsi, M. Hidalgo, S. Legnaioli, V. Palleschi, A. Salvetti, E. Tognoni, S. Green, D. Bates, A. Steiger, J. Fonseca, J. Martins, J. McKay, B. Tozer, D. Wells, R. Wells and M. A. Harith, "Diagnostics of high-temperature steel pipes in industrial environment by laser-induced breakdown spectroscopy technique: the LIBSGRAIN project", Spectrochimica Acta Part B: Atomic Spectroscopy, vol. 57, no. 7, pp. 1181-1192, 2002.

[29] P. García, J. Vadillo and J. Laserna, "Real-Time Monitoring of High-Temperature Corrosion in Stainless Steels by Open-Path Laser-Induced Plasma Spectrometry", Applied Spectroscopy, vol. 58, no. 11, pp. 1347-1352, 11 2004.

[30] G. Vítková, L. Prokeš, K. Novotný, P. Pořízka, J. Novotný, D. Všianský, L. Čelko and J. Kaiser, "Comparative study on fast classification of brick samples by combination of principal component analysis and linear discriminant analysis using stand-off and table-top laser-induced breakdown spectroscopy", Spectrochimica Acta Part B: Atomic Spectroscopy, vol. 101, pp. 191-199, 2014.

[31] J. Novotný, M. Brada, M. Petrilak, D. Prochazka, K. Novotný, A. Hrdlička and J. Kaiser, "A versatile interaction chamber for laser-based spectroscopic applications, with the emphasis on Laser-Induced Breakdown Spectroscopy", Spectrochimica Acta Part B: Atomic Spectroscopy, vol. 101, pp. 149-154, 2014.

[32] T. Labutin, A. Popov, V. Lednev and N. Zorov, "Correlation between properties of a solid sample and laser-induced plasma parameters", Spectrochimica Acta Part B: Atomic Spectroscopy, vol. 64, no. 10, pp. 938-949, 2009.

[33] D. Prochazka, M. Bilík, P. Prochazková, J. Klus, P. Pořízka, J. Novotný, K. Novotný, B. Ticová, A. Bradáč, M. Semela and J. Kaiser, "Detection of tire tread particles using laser-induced breakdown spectroscopy", Spectrochimica Acta Part B: Atomic Spectroscopy, vol. 108, pp. 1-7, 2015.

[34] J. Aguilera and C. Aragón, "Characterization of a laser-induced plasma by spatially resolved spectroscopy of neutral atom and ion emissions", Spectrochimica Acta Part B: Atomic Spectroscopy, vol. 59, no. 12, pp. 1861-1876, 2004.

[35] C. Aragón and J. Aguilera, "Characterization of laser induced plasmas by optical emission spectroscopy: A review of experiments and methods", Spectrochimica Acta Part B: Atomic Spectroscopy, vol. 63, no. 9, pp. 893-916, 2008.

[36] D. Hahn and N. Omenetto, "Laser-Induced Breakdown Spectroscopy (LIBS), Part I: Review of Basic Diagnostics and Plasma–Particle Interactions", Applied Spectroscopy, vol. 64, no. 12, pp. 335-366, 12 2010.

[37] H. Griem, Spectral Line Broadening by Plasmas. Oxford: Elsevier Science, 1974.

[38] A. Kramida, Y. Ralchenko, J. Reader and . NIST ASD Team, "NIST Atomic Spectra Database: (ver. 5.2)", 2014. [Online]. Available: http://physics.nist.gov/asd. [Accessed: 03-04-2015].

This journal is © The Royal Society of Chemistry 20xx